p-ISSN : 2335-1357 e-ISSN : 2437-1122

Mediterranean Journal of Modeling and Simulation

Med. J. Model. Simul. 08 (2017) 019-029

High performance fuzzy sliding mode control of DFIG supplied by seven level NPC inverter

Mohamed BENKAHLA [a] , Rachid TALEB [a] * , Zinelaabidine BOUDJEMA [a]

[a] Electrical Engineering Department, Hassiba Benbouali University. Laboratoire Génie Electrique et Energies Renouvelables (LGEER), Chlef, Algeria

ARTICLE INFO

Article history :
Received September 2016
Accepted August 2017

Keywords :
Doubly fed-induction generator (DFIG) ;
Sliding mode control (SMC) ;
Fuzzy sliding mode control (FSMC) ;
Seven level NPC inverter.

ABSTRACT

This article presents the powers control of a variable speed wind turbine (WT) based on a doubly fed induction generator (DFIG) because of their advantages in terms of economy and control. The considered system consists of a double fed induction generator whose stator is connected directly to the network and its rotor is supplied by seven-level inverter with structure NPC are well used to minimize the harmonics absorbed by the DFIG. In order to control the power flowing between the stator of the DFIG and the grid. Have been studied and compared two types of controllers : Sliding Mode Control (SMC) and Fuzzy SMC (FSMC). Their respective performances are compared in terms of power reference tracking, response to sudden speed variations, sensitivity to perturbations and robustness against machine parameters variations.

1. Introduction

Wind power has developed significantly during the past few years. However, its usage poses great challenges to operation and control of power systems. Doubly fed induction generator (DFIG) has gained increasing popularity in wind power generation recently due to its flexible controllability [1]. DFIG comprises a wound rotor induction generator supplied on the stator side by the grid connection and on the rotor side by a power electronic converter [2]. The stator is directly connected to the grid and the rotor is fed to magnetize the machine.

The seven level NPC inverter is used in the domains of high voltage and strong power. We develop his model of order within the meaning of the average values by using the notion of generating functions. A control strategy of this inverter is developed. The performances of this algorithm are analyzed on the basis of the characteristic of regulating and the rate

*Email : rac.taleb@gmail.com

of harmonic. A knowledge model of this converter using switching functions and a SPWM strategy is detailed. For an economic point of view, the objective is to use the proposed inverter on seven levels in order to minimize the harmonics absorbed by the DFIG.

Recently, the sliding mode control (SMC) method has been widely used for robust control of nonlinear systems. Several papers have been published based on (SMC) of DFIG [3, 4]. The SMC achieves robust control by adding a discontinuous control signal across the sliding surface, satisfying the sliding condition. Nevertheless, this type of control has an essential disadvantage, which is the chattering phenomenon caused by the discontinuous control action.

To treat these difficulties, several modifications to the original sliding control law have been proposed, the most popular being the boundary layer approach [5, 6].

Fuzzy logic is a technology based on engineering experience and observations. In fuzzy logic, an exact mathematical model is not necessary because linguistic variables are used to define system behavior rapidly. One way to improve sliding mode controller performance is to combine it with fuzzy logic to form a fuzzy sliding mode controller (FSMC). The design of a sliding mode controller incorporating fuzzy control helps in achieving reduced chattering, simple rule base, and robustness against disturbances and nonlinearities.

The paper is structured as follows : system modeling (WT, seven level NPC inverter and DFIG) is discussed in Section 2. In Section 3, the control strategies of the DFIG is presented. Session 4 shows the simulation results of the DFIG using two different nonlinear controllers ; sliding mode, fuzzy sliding mode. Finally, in section 5 the main conclusions of the work are drawn.

2. System modeling

2.1. Wind turbine model

For a horizontal axis wind turbine, the output mechanical power extracted from the wind is given by [7].

$$P_t = \frac{1}{2} C_P(\lambda, \beta) R^2 \rho v^3 \tag{1}$$

where, C_P is the power coefficient which is a function of both tip speed ratio λ, and blade pitch angle β (deg), and ν is the wind speed (m/s), ρ is the air density (kg/m^3), and R is the radius of the turbine (m). In this work, the C_P equation is approximated using a non-linear function according to [8].

$$C_P = (0.5 - 0.167)(\beta - 2)\sin\left[\frac{\pi(\lambda + 0.1)}{18.5 - 0.3(\beta - 2)}\right] - 0.0018(\lambda - 3)(\beta - 2) \tag{2}$$

the tip speed ratio is given by :

$$\lambda = \frac{\Omega_t R}{\nu} \tag{3}$$

2.2. Modeling of the inverter on seven levels with structure NPC

The three-phase inverter on seven levels with structure NPC is a new structure of conversion used to feed, to tension and frequency variables, of motors to alternating

current of strong power. Within the framework of our work, we present a structure of the inverter seven NPC type levels as shown in Fig. 1.

The function of connection (F_{KS}) of each switch described its closed or open state. This function is defined like continuation :

$$F_{KS} = \begin{cases} 1 \text{ if } TD_{KS} \text{ isclosed} \\ 0 \text{ if } TD_{KS} \text{ isopen} \end{cases} \tag{4}$$

One defines for the inverter a function of connection of the half-arm, which one will note F_{km}^{b} such as :

$$m = \begin{cases} 0 \text{ for the half} - \text{arm of the low} \\ 1 \text{ for the half} - \text{arm of the high} \end{cases} \tag{5}$$

K : Number of the arm $K = (1, 2, 3)$

The output voltages of the three-phase inverter on seven levels relatively to the middle point M express themselves as follows :

$$\begin{aligned} \begin{bmatrix} V_{AM} \\ V_{BM} \\ V_{BM} \end{bmatrix} = & \begin{bmatrix} F_{111} + F_{112} + F_{11}^{b} \\ F_{211} + F_{212} + F_{21}^{b} \\ F_{311} + F_{312} + F_{31}^{b} \end{bmatrix} U_{C1} + \begin{bmatrix} F_{112} + F_{11}^{b} \\ F_{212} + F_{21}^{b} \\ F_{312} + F_{31}^{b} \end{bmatrix} U_{C2} + \begin{bmatrix} F_{11}^{b} \\ F_{21}^{b} \\ F_{31}^{b} \end{bmatrix} U_{C3} \\ & - \begin{bmatrix} F_{113} + F_{114} + F_{10}^{b} \\ F_{213} + F_{214} + F_{20}^{b} \\ F_{313} + F_{314} + F_{30}^{b} \end{bmatrix} U_{C4} - \begin{bmatrix} F_{114} + F_{10}^{b} \\ F_{214} + F_{20}^{b} \\ F_{314} + F_{30}^{b} \end{bmatrix} U_{C5} - \begin{bmatrix} F_{10}^{b} \\ F_{20}^{b} \\ F_{30}^{b} \end{bmatrix} U_{C6} \end{aligned} \tag{6}$$

For the simple tensions, we have :

$$\begin{aligned} V_A &= V_{AN} = V_{AM} - V_{NM} \\ V_B &= V_{BN} = V_{BM} - V_{NM} \\ V_C &= V_{CN} = V_{CM} - V_{NM} \end{aligned} \tag{7}$$

$$V_{NM} = \frac{1}{3}\left(V_{AM} + V_{BM} + V_{CM}\right) \tag{8}$$

From the relations (7) and (8), we have :

$$\begin{aligned} V_A &= V_{AM} - \tfrac{1}{3}\left(V_{AM} + V_{BM} + V_{CM}\right) = \tfrac{1}{3}\left(2V_{AM} - V_{BM} - V_{CM}\right) \\ V_B &= V_{BM} - \tfrac{1}{3}\left(V_{AM} + V_{BM} + V_{CM}\right) = \tfrac{1}{3}\left(-V_{AM} + 2V_{BM} - V_{CM}\right) \\ V_C &= V_{CM} - \tfrac{1}{3}\left(V_{AM} + V_{BM} + V_{CM}\right) = \tfrac{1}{3}\left(-V_{AM} - V_{BM} + 2V_{CM}\right) \end{aligned} \tag{9}$$

From relationships (6) and (9), one obtains the matrix system giving the expressions of the voltages across the load following :

$$\begin{bmatrix} V_A \\ V_B \\ V_C \end{bmatrix} = \frac{1}{3}\begin{bmatrix} 2 & -1 & -1 \\ -1 & 2 & -1 \\ 2 & -1 & 2 \end{bmatrix}\left\{ \begin{bmatrix} F_{111}+F_{112}+F_{11}^b \\ F_{211}+F_{212}+F_{21}^b \\ F_{311}+F_{312}+F_{31}^b \end{bmatrix} U_{C1} + \begin{bmatrix} F_{112}+F_{11}^b \\ F_{212}+F_{21}^b \\ F_{312}+F_{31}^b \end{bmatrix} U_{C2} + \begin{bmatrix} F_{11}^b \\ F_{21}^b \\ F_{31}^b \end{bmatrix} U_{C3} - \begin{bmatrix} F_{113}+F_{114}+F_{10}^b \\ F_{213}+F_{214}+F_{20}^b \\ F_{313}+F_{314}+F_{30}^b \end{bmatrix} U_{C4} - \begin{bmatrix} F_{114}+F_{10}^b \\ F_{214}+F_{20}^b \\ F_{314}+F_{30}^b \end{bmatrix} U_{C5} - \begin{bmatrix} F_{10}^b \\ F_{20}^b \\ F_{30}^b \end{bmatrix} U_{C6} \right\} \tag{10}$$

if one takes into consideration the following hypothesis :

$$U_{C1} = U_{C2} = U_{C3} = U_{C4} = U_{C5} = U_{C6} = U_C$$

this relation is reduced to :

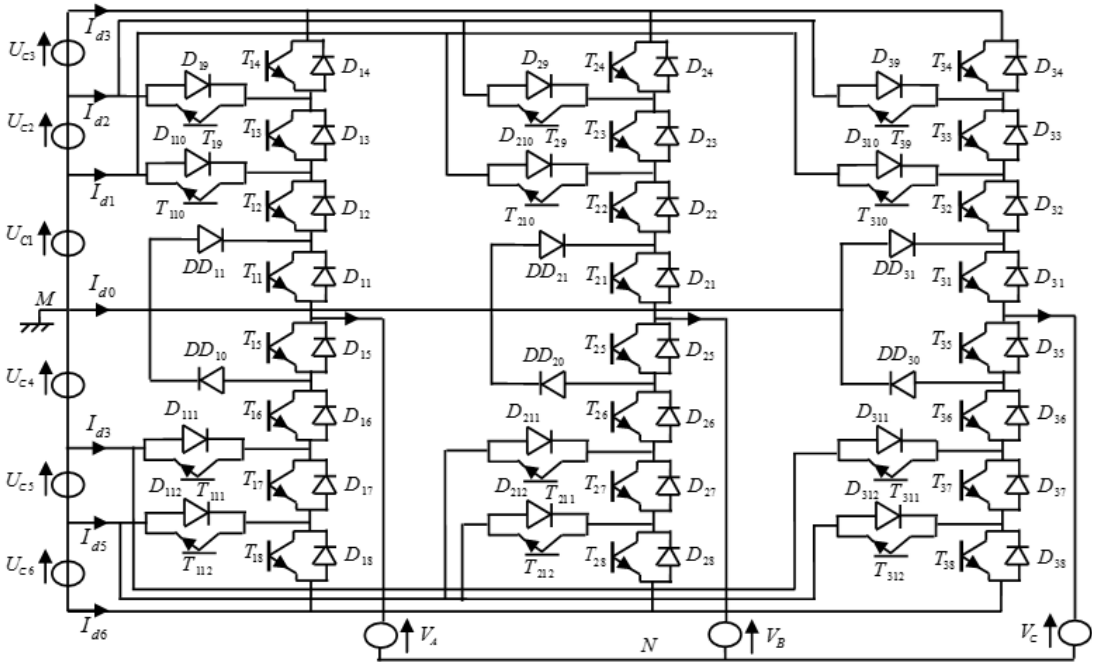

Fig. 1 – Seven Level NPC Voltage Source Inverter.

$$\begin{bmatrix} V_A \\ V_B \\ V_C \end{bmatrix} = \begin{bmatrix} 2 & -1 & -1 \\ -1 & 2 & -1 \\ -1 & -1 & 2 \end{bmatrix}\begin{bmatrix} F_{111}+2F_{112}+3F_{11}^b-F_{113}-2F_{114}-3F_{10}^b \\ F_{211}+2F_{212}+3F_{21}^b-F_{213}-2F_{214}-3F_{20}^b \\ F_{311}+2F_{312}+3F_{31}^b-F_{313}-2F_{314}-3F_{30}^b \end{bmatrix} U_C \tag{11}$$

2.3. The DFIG model

The dynamic voltages and fluxes equations of the DFIG in the synchronous d-q reference frame are given by :

$$\begin{cases} V_{ds} = R_s I_{ds} + \frac{d}{dt}\Psi_{ds} - \omega_s \Psi_{qs} \\ V_{qs} = R_s I_{qs} + \frac{d}{dt}\Psi_{qs} - \omega_s \Psi_{ds} \\ V_{dr} = R_r I_{dr} + \frac{d}{dt}\Psi_{dr} - \omega_r \Psi_{qr} \\ V_{qr} = R_r I_{dr} + \frac{d}{dt}\Psi_{qr} - \omega_r \Psi_{dr} \end{cases}, \quad \begin{cases} \psi_{ds} = L_s I_{ds} + M I_{dr} \\ \psi_{qs} = L_s I_{qs} + M I_{qr} \\ \psi_{dr} = L_r I_{dr} + M I_{ds} \\ \psi_{qr} = L_r I_{qr} + M I_{qs} \end{cases} \tag{12}$$

The powers at the stator side are expressed as follows [2] :

$$\begin{cases} P_s = -\frac{\omega_s \psi_s M}{L_s} I_{qr} \\ Q_s = -\frac{\omega_s \psi_s M}{L_s} I_{dr} + \frac{\omega_s {\psi_s}^2}{L_s} \end{cases} \tag{13}$$

3. Control strategies of the DFIG

In this section, comparison of DFIG performances using different nonlinear controllers : sliding mode and fuzzy sliding mode, has been presented.

3.1. Sliding mode control

The main feature of this control is that it only needs to drive the error to a "switching surface". In this study, the errors between the measured and references stator powers have been chosen as sliding mode surfaces, so the following expression can be written [9] :

$$\begin{cases} S_d = P_{s\_ref} - P_s \\ S_q = Q_{s\_ref} - Q_s \end{cases} \tag{14}$$

the first derivative of (14), gives :

$$\begin{cases} \dot{S}_d = \dot{P}_{S-ref} - \dot{P}_S \\ \dot{S}_q = \dot{Q}_{S-ref} - \dot{Q}_S \end{cases} \tag{15}$$

replacing the powers in (15) by their expressions given in (13), we obtains :

$$\begin{cases} \dot{S}_d = \dot{P}_{S-ref} - \frac{\omega_s \psi_s M}{L_s} \dot{I}_{qr} \\ \dot{S}_q = \dot{Q}_{S-ref} - \frac{\omega_s \psi_s M}{L_s} \dot{I}_{dr} - \frac{\omega_s \psi_s^2}{L_s} \end{cases} \tag{16}$$

V_{dr} and V_{qr} will be the two components of the control vector used to constraint the system to converge to $S_{dq} = 0$. The control vector V_{dqeq} is obtained by imposing $\dot{S}_{dq} = 0$:

$$V_{eqdq} = \begin{bmatrix} -\frac{L_s\left(L_r - \frac{M^2}{L_s}\right)}{\omega_s \psi_s M} \dot{Q}_s^* + R_r I_{dr} - \left(L_r - \frac{M^2}{L_s}\right) g \omega_s I_{qr} + \frac{\left(L_r - \frac{M^2}{L_s}\right) \psi_s}{M} \\ \frac{L_s}{\omega_s \psi_s M} \dot{P}_s^* + R_r I_{qr} - \left(L_r - \frac{M^2}{L_s}\right) g \omega_s I_{dr} + \frac{g \omega_s \psi_s M}{L_s} \end{bmatrix} \tag{17}$$

To obtain good performances, dynamic and commutations around the surfaces, the control vector is imposed as follows :

$$V_{dq} = V_{eqdq} + K.sat\left(S_{dq}\right) \tag{18}$$

The sliding mode will exist only if the following condition is verified : $S \cdot \dot{S} < 0$

The block diagram of the active and reactive powers sliding mode control applied to the DFIG is shown in Fig. 2.

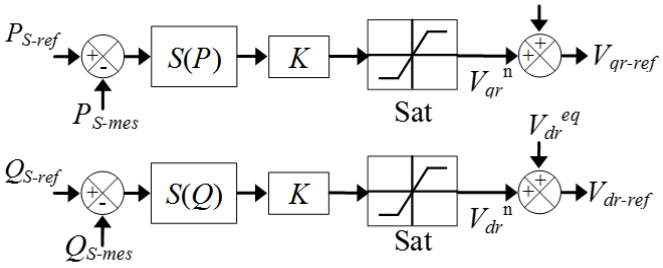

Fig. 2 – Block diagram of the sliding mode controller.

3.2. Fuzzy sliding mode control of the DFIG

The disadvantage of sliding mode controllers is the chattering effect. In order to eliminate this phenomenon, a fuzzy sliding mode control method has been proposed. The fuzzy sliding mode controller (FSMC) is a modification of the sliding mode controller, where the switching controller term $sat(S(x))$, has been replaced by a fuzzy control input as given below [10]. Is shown in Fig. 3,

$$U^{com} = U^{eq} + U^{Fuzzy} \tag{19}$$

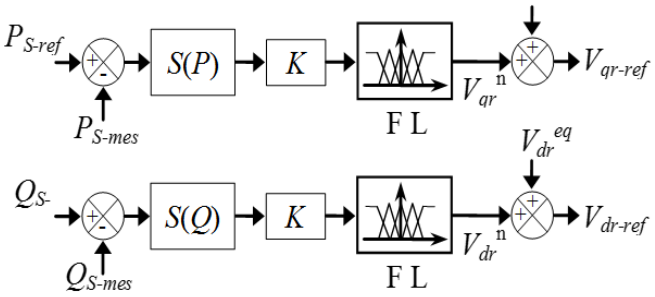

Fig. 3 – Block diagram of the fuzzy sliding mode controller.

4. Simulation results and discussions

In this section, simulations are realized with a 7.5 KW generator coupled to a 380V/50Hz grid. Parameters of the machine are given in table 1. In the aim to evaluate the performances of the two controllers SMC and FSMC, three categories of tests have been realized : pursuit test, sensitivity to the speed variation and robustness against machine parameter variations.

Table 1 – Machine parameters.

Parameters	**Rated Value**	**Unity**
Nominal power	7.5	KW
Stator voltage	380	V
Stator frequency	50	Hz
Number of pairs poles	2	
Nominal speed	150	rad/s
Stator resistance	1.2	Ω
Rotor resistance	0.62	Ω
Stator inductance	0.084	H
Rotor inductance	0.081	H
Mutual inductance	0.078	H
Inertia	0.01	$Kg.m^2$

4.1. Pursuit test

This test has for goal the study of the three controller's behaviors in reference tracking, while the machine's speed is considered constant and equal to its nominal value. The simulation results are presented in Fig. 4 and Fig. 5, As it's shown by Fig. 4, for the two controllers, the active and reactive generated powers tracks almost perfectly their references and ensures a perfect decoupling between the two axes. Therefore it can be considered that the three types of controllers have a very good performance for this test. On the other hand, Fig. 5 shows the harmonic spectrum of one phase stator current of the DFIG obtained using Fast Fourier Transform (FFT) technique for the three controllers. It can be clear observed that the total harmonic distortion (THD) is reduced for FSMC supplied by seven-level inverter with structure NPC (THD=1.29%) when compared to FSMC (THD=1.93%) and SMC (THD=2.06%) supplied by two-level inverter.

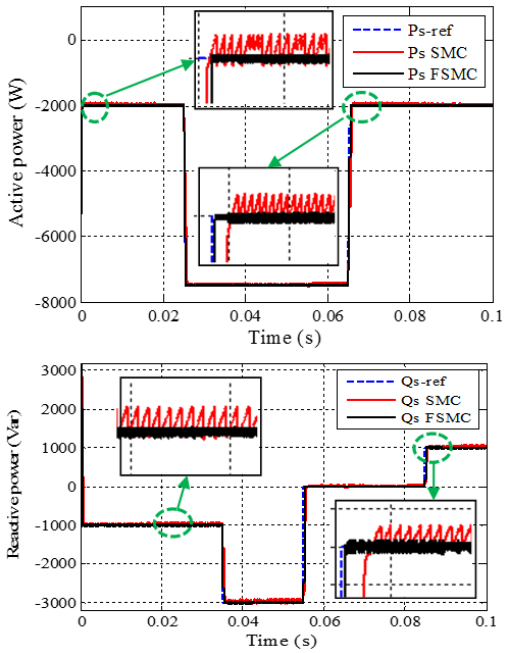

Fig. 4 – Reference tracking test.

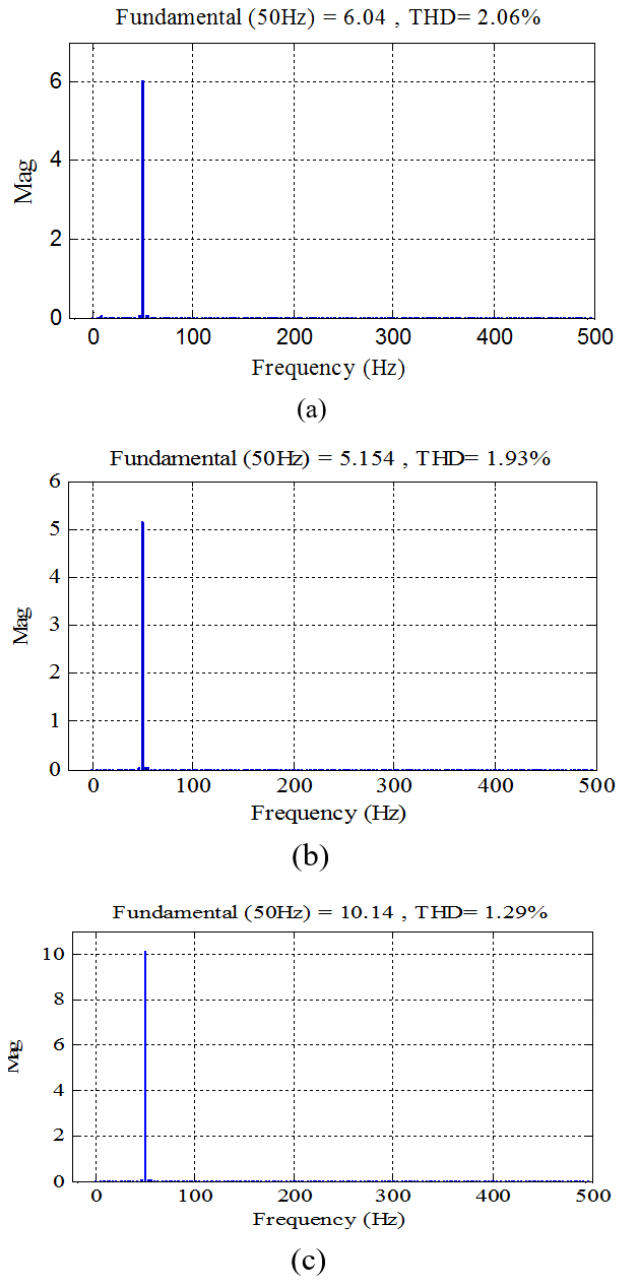

Fig. 5 – Spectrum harmonic of one phase stator current for : (a) SMC supplied by a two-level inverter, (b) FSMC supplied by a two-level inverter and (c) for FSMC supplied by a seven-level inverter.

4.2. Sensitivity to the speed variation

The goal of this test is to analyze the influence of a speed variation of the DFIG on reactive and active powers for two controllers. For this objective and at time=0.04s, the speed was varied from 150 rad/s to 170 rad/s shown in Fig. 6, The simulation results are shown in Fig. 7, This figure express that the speed variation produced a slight effect on the powers curves of the system with SMC controller, while effect is almost negligible for the system with FSMC one. It can be noticed that this last has a nearly perfect speed disturbance rejection, indeed ; only very small power variation can be observed (fewer than

2%). This result is attractive for wind energy application quality and to ensure stability of the generated power when the sped is varying.

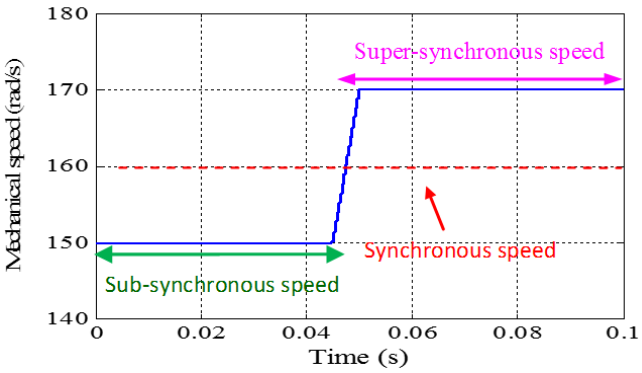

Fig. 6 – Mechanical speed profile.

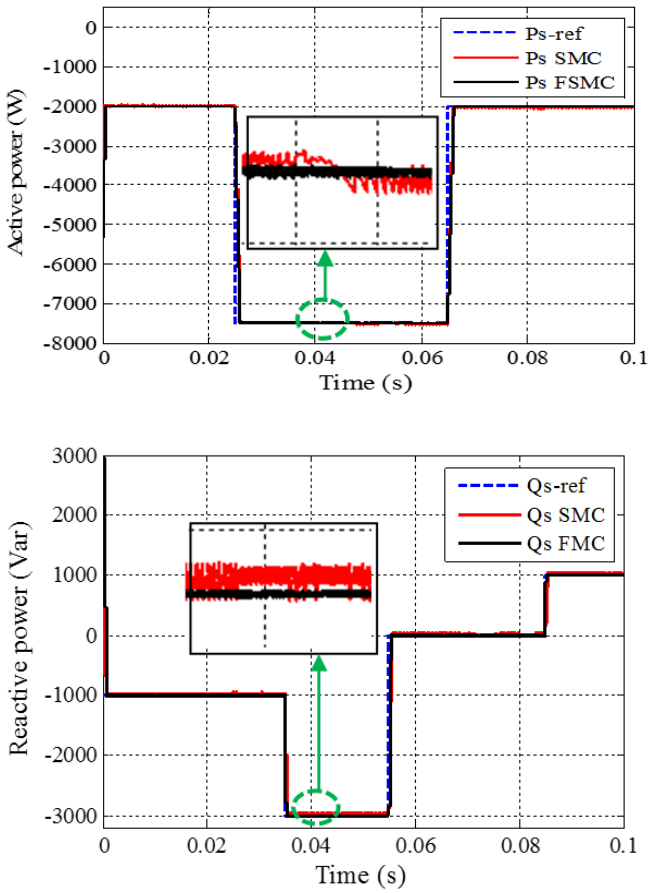

Fig. 7 – Sensitivity to the speed variation.

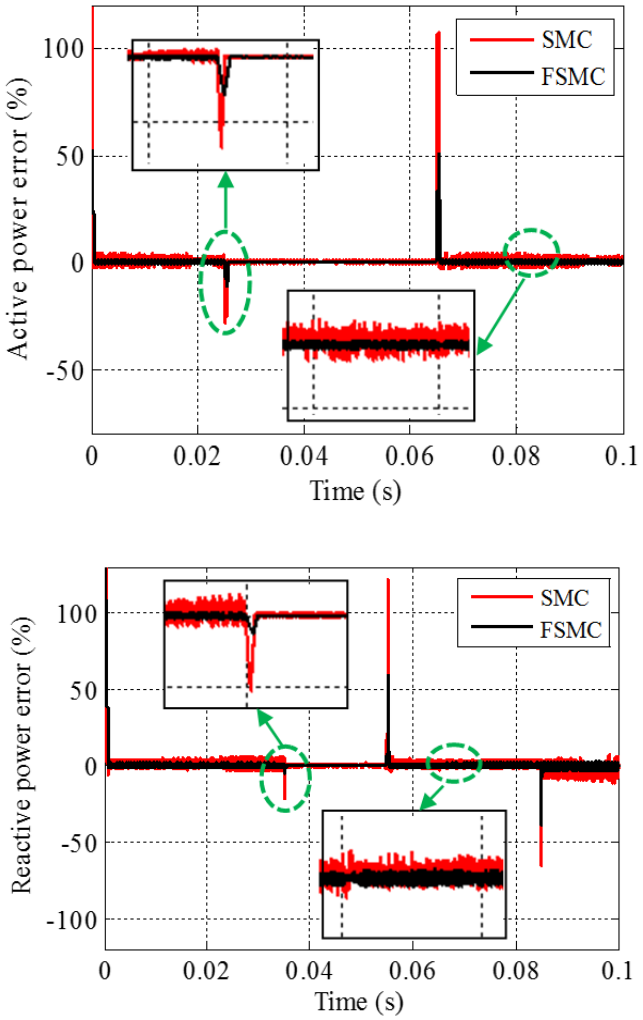

Fig. 8 – Effect machine's parameters variation on the robust control.

4.3. Robustness tests

The aim of these tests is to analyze the influence of the DFIG's parameters variation on the controllers' performance. The DFIG is running at its nominal speed, to test the robustness of the controllers used, parameters of the machine. have been modified : the values of the rotor and stator resistances R_r and R_s are multiplied by 2, while the values of inductances L_s, L_r and M are divided by 2, the obtained results are presented in Fig. 8, These results show that parameters variation of the DFIG presents a clear effect on the powers curves (especially in their errors curves) and that the effect appears more significant for SMC controller than that with FSMC one. Thus it can be concluded that this last is the most robust among the proposed controllers studied in this work.

5. Conclusion

The modeling, the simulation and the control of an electrical power conversion system based on a DFIG connected directly to the grid by the stator and fed by seven-level inverter with structure NPC on the rotor side has been presented in this article. Our objective was the implementation of a fuzzy sliding mode control method of active and

reactive powers generated by the stator side of the DFIG, in order to ensure of the high performance and a better execution of the DFIG, and to make the system insensible with the external disturbances and the parametric variations. In the first step, we started with a study of modeling on the seven-level inverter with structure NPC controlled by the SPWM, because this later present it ensures a highest quality torque and to minimize the current Harmonics. . In second step, we adopted a vector control strategy in order to control active and reactive power exchanged between the stator of the DFIG and the grid. In third step, the description of the classical sliding mode controller (SMC) is presented in detail. Then, the fuzzy logic control is used to mimic the hitting control law to remove the chattering. Compared with the conventional sliding mode controller, the fuzzy sliding mode control system results in robust control performance without chattering. The chattering free improved performance of the FSMC makes it superior to conventional SMC, and establishes its suitability for the system drive.

REFERENCES

[1] P. B. Eriksen, T. Ackermann, H. Abildgaard, P. Smith, W. Winter, and J. M. Rodriguez Garcia, "System operation with high wind penetration," IEEE Power Energy Manag, vol. 3, no. 6, pp. 65-74, 2005.

[2] G. Pannell, D. Atkinson, B. Zahawi, "Analytical Study of Grid-Fault Response of Wind Turbine Doubly Fed Induction Generator," IEEE Transactions on Energy Conversion, vol. 25, no. 4, 2010, pp. 1081-1091.

[3] Martinez, M. I., Tapia, G., Susperregui, A., and Camblong, H. : "Sliding-mode control for DFIG rotor and grid-side converters under unbalanced and harmonically distorted grid voltage," IEEE Trans. On Energy Conversion, Vol. 27, No. 2, pp. 328-339, March 2000.

[4] Hu, J., Nian, H., Hu, B., He, Y. and Zhu, Z. Q. : "Direct active and reactive power regulation of DFIG using sliding-mode control approach," IEEE Trans. On Energy Conversion, Vol. 25, No. 4, pp. 1028–1039, Dec. 2010.

[5] Lopez, J., Sanchis, P., Roboam, X., Marroyo, L. : "Dynamic behavior of the doubly fed induction generator during three-phase voltage dips," IEEE Transaction on Energy Conversion, pp. 709-717, 22 (September (3)) 2007.

[6] Cupertino, F., Naso, D., Mininno, E., Turchiano, B. : "Sliding-mode control with double boundary layer for robust compensation of payload mass and friction in linear motors," IEEE Trans. On Industry Applications, Vol. 45, No. 5, pp. 1688-1696, Sep./Oct 2009.

[7] Y. Zou, M. E. Elbuluk, Y. Sozer, "Stability analysis of maximum power point tracking (MPPT) method in wind power systems," IEEE Transactions on Industry Applications, vol. 49, No. 3, pp. 1129- 1136, 2013.

[8] E. S. Abdin, W. Xu, "Control design and Dynamic Performance Analysis of a Wind Turbine Induction Generator Unit," IEEE Transactions on Energy Conversion, vol. 15, No. 1, pp. 91 – 96, March 2000.

[9] Z. Yan, C. Jin, V.I. Utkin, "Sensorless sliding mode control of induction motors," IEEE Trans. Ind. electronic. 47 (2000).

[10] L.K. Wong, F.H.F. Leung, P.K.S. Tam, "A fuzzy sliding controller for nonlinear systems," IEEE Trans. Ind. electronic, 48 (2001).